Comp. Meth. Civil Eng., Vol. 3, 1 (2012) 63-76

CMCE
Computational Methods in Civil Engineering

Equilibrium condition nonlinear modeling of a cracked concrete beam using a 2D Galerkin finite volume solver

S.R. Sabbagh Yazdi[a *], M. Bayatlou[b]

[a] *Professor of Civil Engineering Department of KNToosi University of Technology*
[b] *Postgraduate of Civil Engineering Department of KNToosi University of Technology*

Received 6 March 2012; accepted in revised form 24 October 2012

Abstract

A constitutive model based on two–dimensional unstructured Galerkin finite volume method (GFVM) is introduced and applied for analyzing nonlinear behavior of cracked concrete structures in equilibrium condition. The developed iterative solver treats concrete as an orthotropic nonlinear material and considers the softening and hardening behavior of concrete under compression and tension by using two equivalent uniaxial stress–strain relations. The concepts of current strength in a principal stress space and secant stiffness matrix are utilized to describe the biaxial behavior of concrete and the post–peak progress of stress–strain relation is modeled using the fracture energy method. Moreover, a smeared rotating crack method (SRCM) formulation is implemented in the solver to spot the nonlinear behavior of damaged structure. In order to demonstrate the performance of the model at a structural level, available experimental results of a notched beam under three point bending are presented. With the intention of demonstrating the post–peak performance of the model, the procedure of loading is simulated by imposing an incremental monotonic displacement. The envelope curve of equivalent load versus crack mouth opening displacement (CMOD) is utilized to evaluate the accuracy of the introduced method.

Keywords: Iterative Galerkin finite volume method; Smeared rotating crack method; Cracked concrete softening and hardening; Equilibrium condition.

1. Introduction

During the recent decades and by the advances in micro processing technologies, reliability and applicability of numerical analysis have increased significantly. In this regard, finite volume method (FVM) has earned a great reputation, especially in the field of computational fluid dynamics (CFD) [1], heat and mass transfer calculations [2]. Nowadays, according to the high potentials of this method, mainly in considering large displacements, researchers show interest in using FVM for computational solid mechanics (CSM) [3].

*Corresponding author.
E-mail address: SYazdi@kntu.ac.ir

Previously, finite element method (FEM) was the undisputed approach in the field of CSM, especially with regard to deformation problems involving nonlinear material analysis [1], but since FEM could face some difficulties such as volumetric locking in dealing with excessive displacements [2], the interest in using FVM as an alternative solution method has increased. Unlike finite difference method (FDM) [4] which solve partial differential equation(s) of the desired problem on a set of grid points, FVM integrates the governing equation(s) over pre–defined sub–domains [2]. Similar to the FEM, some schemes of the FVM have been developed for solving mathematical models on unstructured meshes. So, modeling of geometrical complexities of real world problems and the refinement of grid spacing in the regions with high gradient of dependent variables are possible via FVM solution procedure. Galerkin finite volume method (GFVM) is among various schemes of FVMs which are introduced based on the procedure of defining sub–domains and integrating governing equation(s). GFVM is an overlapping vertex based method which utilizes the Galerkin's weighted residuals concept and linear shape function of triangular and tetrahedral elements in two-dimensional (2D) and three-dimensional (3D) spaces, respectively [5].

On the other hand, the concept of smeared rotating crack method (SRCM) which is developed from crack band theory [6] is in total coordination with GFVM. Utilizing SCM in modeling the behavior of concrete under excessive tension and compression proved to be practical [7]. In the present paper, the nonlinear behavior of cracked concrete and evolution of crushes through the material is modeled by developing a GFVM numerical solver based on SRCM concept.

2. Governing equations

Based on the concept of SRCM, the iterative process of predicting the nonlinear behavior of concrete is divided into two major parts. The first part employs linear–elastic formulation to model the linear behavior of solid materials, while the second part contains an appropriate model which could alter the properties of the material by using the criteria related to nonlinear behavior of concrete.

2.1. Linear–elastic formulation

The general mathematical model for continuum mechanics in the absence body forces can be defined by Cauchy's equilibrium equations.

$$\rho\ddot{u} = S^T\sigma + b \ , \tag{1}$$

where, ρ is the material density, $\ddot{u}$ is the acceleration, σ is the stress tensor and b is the body force.

For 2D problems and in *x–y* coordinates system, stress tensor would take the form of $\sigma_{xy} = [\sigma_x \quad \sigma_y \quad \tau_{xy}]^T$. The acceleration vector is obtained from displacement vector $\vec{u} = [u_x \quad u_y]^T$ and operator S^T is defined as

$$S^T = \begin{bmatrix} \frac{\partial}{\partial x} & 0 & \frac{\partial}{\partial y} \\ 0 & \frac{\partial}{\partial y} & \frac{\partial}{\partial x} \end{bmatrix}. \tag{2}$$

So the matrix form of Cauchy's equilibrium equations in 2D *x–y* coordinates system is

$$\rho \begin{Bmatrix} \frac{\partial^2 u_x}{\partial t^2} \\ \frac{\partial^2 u_y}{\partial t^2} \end{Bmatrix} = \begin{bmatrix} \frac{\partial}{\partial x} & 0 & \frac{\partial}{\partial y} \\ 0 & \frac{\partial}{\partial y} & \frac{\partial}{\partial x} \end{bmatrix} \begin{Bmatrix} \sigma_x \\ \sigma_y \\ \tau_{xy} \end{Bmatrix} \tag{3}$$

For stress–strain relation, the common relations can be used as

$$\sigma_{xy} = \boldsymbol{D}_{xy}\varepsilon_{xy} \ , \tag{4}$$

where, $\varepsilon_{xy} = [\varepsilon_{xx} \quad \varepsilon_{yy} \quad \gamma_{xy}]^T$ is the strain tensor and D_{xy} is the 2D stiffness matrix which takes the following form,

$$\boldsymbol{D}_{xy} = \begin{bmatrix} D_{xy_{(1,1)}} & D_{xy_{(1,2)}} & D_{xy_{(1,3)}} \\ \vdots & D_{xy_{(2,2)}} & D_{xy_{(2,3)}} \\ Symmetry & \dots & D_{xy_{(3,3)}} \end{bmatrix}. \tag{5}$$

So stress–strain relation is defined as

$$\begin{aligned} \sigma_{xx} &= D_{xy_{(1,1)}}\varepsilon_{xx} + D_{xy_{(1,2)}}\varepsilon_{yy} + D_{xy_{(1,3)}}\gamma_{xy}, \\ \sigma_{yy} &= D_{xy_{(1,2)}}\varepsilon_{xx} + D_{xy_{(2,2)}}\varepsilon_{yy} + D_{xy_{(2,3)}}\gamma_{xy}, \\ \tau_{xy} &= \tau_{yx} = D_{xy_{(1,3)}}\varepsilon_{x} + D_{xy_{(2,3)}}\varepsilon_{y} + D_{xy_{(3,3)}}\gamma_{xy}. \end{aligned} \tag{6}$$

Considering the elastic behavior of material, the strains could be replaced by

$$\varepsilon_{xx} = \frac{\partial u_x}{\partial x}, \quad \varepsilon_{yy} = \frac{\partial u_y}{\partial y}, \quad \gamma_{xy} = \frac{\partial u_x}{\partial y} + \frac{\partial u_y}{\partial x} \ . \tag{7}$$

So the Cauchy's equilibrium equations in two Cartesian coordinate directions take the form,

$$\begin{aligned} \boldsymbol{\rho}\frac{\boldsymbol{\partial^2 u_x}}{\boldsymbol{\partial t^2}} &= \frac{\partial}{\partial x}\overbrace{\left[C_1\left(\frac{\partial u_x}{\partial x}\right) + C_2\left(\frac{\partial u_y}{\partial y}\right) + C_3\left(\frac{\partial u_x}{\partial y} + \frac{\partial u_y}{\partial x}\right)\right]}^{\boldsymbol{\sigma_{xx}}} \\ &\quad + \frac{\partial}{\partial y}\overbrace{\left[C_3\left(\frac{\partial u_x}{\partial x}\right) + C_5\left(\frac{\partial u_y}{\partial y}\right) + C_6\left(\frac{\partial u_x}{\partial y} + \frac{\partial u_y}{\partial x}\right)\right]}^{\boldsymbol{\tau_{xy}}} \end{aligned} \tag{8}$$

$$\begin{aligned} \boldsymbol{\rho}\frac{\boldsymbol{\partial^2 u_y}}{\boldsymbol{\partial t^2}} &= \frac{\partial}{\partial y}\overbrace{\left[C_2\left(\frac{\partial u_x}{\partial x}\right) + C_4\left(\frac{\partial u_y}{\partial y}\right) + C_5\left(\frac{\partial u_x}{\partial y} + \frac{\partial u_y}{\partial x}\right)\right]}^{\boldsymbol{\sigma_{yy}}} \\ &\quad + \frac{\partial}{\partial x}\overbrace{\left[C_3\left(\frac{\partial u_x}{\partial x}\right) + C_5\left(\frac{\partial u_y}{\partial y}\right) + C_6\left(\frac{\partial u_x}{\partial y} + \frac{\partial u_y}{\partial x}\right)\right]}^{\boldsymbol{\tau_{xy}}} \end{aligned} \tag{9}$$

where, coefficients $C_1 \ to \ C_6$ are

$$\begin{aligned} &C_1 = D_{xy_{(1,1)}}, \quad C_2 = D_{xy_{(1,2)}}, \quad C_3 = D_{xy_{(1,3)}}, \\ &C_4 = D_{xy_{(2,2)}}, \quad C_5 = D_{xy_{(2,3)}}, \quad C_6 = D_{xy_{(3,3)}}. \end{aligned} \tag{10}$$

2.2. Nonlinear formulation

In general, when a principal stress exceeds the material's strength, the material cracks or crushes perpendicular to the direction of the principal stress. Hence, the isotropic stress–strain relations can be replaced by an orthotropic law.

The proposed model in this paper, utilizes the SRCM concept [6] to represents the damaged (cracked or crushed) concrete as an orthotropic material. It's assumed that the directions of the principal stresses and those of the principal strains in the concrete remain coincident [8].

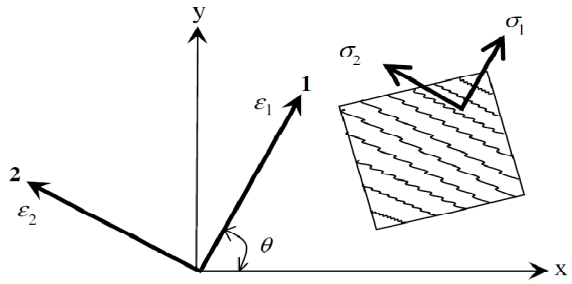

Figure 1. Smeared rotating crack model [7].

In the SRCM (see Figure 1), the orthotropic stress–strain relations are defined as [6,7]

$$\sigma_{12} = \boldsymbol{D}_{12}\varepsilon_{12} \tag{11}$$

where,

$$\sigma_{12} = [\sigma_1 \quad \sigma_2 \quad \tau_{12}]^T , \tag{12}$$

$$\varepsilon_{12} = [\varepsilon_1 \quad \varepsilon_2 \quad \gamma_{12}]^T , \tag{13}$$

and D_{12} is the secant stiffness matrix [7] which is defined in section 2.2.4. The relation between ε_{12} in the 1–2 coordinates system (which correspond to the principal directions) and ε_{xy} in the global *x*–*y* coordinates system is given as

$$\varepsilon_{12} = \boldsymbol{T}_\varepsilon(\theta)\varepsilon_{xy} . \tag{14}$$

The transformation matrix $T_\varepsilon(\theta)$ is given in the form

$$\boldsymbol{T}_\varepsilon(\theta) = \begin{bmatrix} C_{x1}^2 & C_{y1}^2 & C_{x1}C_{y1} \\ C_{x2}^2 & C_{y2}^2 & C_{x2}C_{y2} \\ 2C_{x1}C_{x2} & 2C_{y1}C_{y2} & C_{x1}C_{y2} + C_{x2}C_{y1} \end{bmatrix}, \tag{15}$$

in which, $C_{ij} = Cos(\theta_{ij})$, is the cosine between the i axis and the j axis. Through coordinate transformation, the secant stiffness matrix D_{xy} in the global *x*–*y* coordinates system can be expressed as

$$\boldsymbol{D}_{xy} = \boldsymbol{T}_\varepsilon^T(\theta)\boldsymbol{D}_{12}\boldsymbol{T}_\varepsilon(\theta) . \tag{16}$$

Finally, the stress vector σ_{xy} in the global *x*–*y* coordinates system is given by

$$\sigma_{xy} = \boldsymbol{T}_\varepsilon^T(\theta)\sigma_{12} . \tag{17}$$

2.2.1. Current strength

The strength of concrete under multi–axial stresses cannot be predicted using the uniaxial tensile and compressive strengths. Therefore, when concrete is subjected to biaxial stresses, it is important to define the strength of concrete as a function of the stress state.

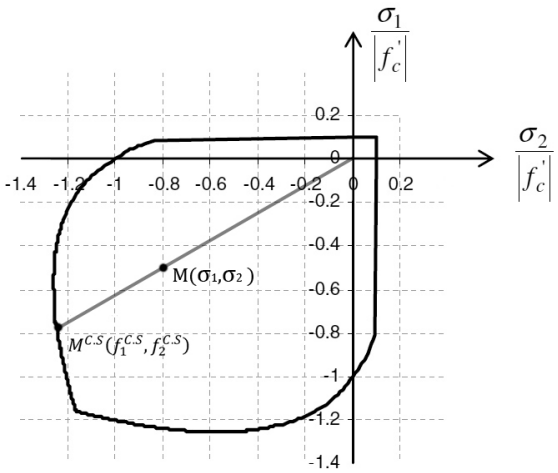

Figure 2. Ultimate strength envelope of concrete under biaxial stresses [6].

To reproduce the important two–dimensional strength characteristics of the laboratory experimental results, as shown in Figure 2, the current strength of concrete is determined using an ultimate strength envelope [9].

In the compression–compression stress state, the ultimate strength envelope is described by the following relation

$$\begin{cases} f_2^{C.S} = \frac{1+3.65\beta}{(1+\beta)^2} f_c' \\ f_1^{C.S} = \beta f_2^{C.S} \end{cases} \quad ; \quad \sigma_1 \le 0, \quad \sigma_2 < 0 \ , \tag{18}$$

where, f_c' is the uniaxial compressive strength of concrete and $\beta = \sigma_1/\sigma_2$ is the current principal stress ratio. The super-script C.S stands for concrete stress.

In the tension–tension stress state, the ultimate strength envelope is given as

$$\begin{cases} f_1^{C.S} = f_t \\ f_2^{C.S} = f_t \end{cases} \quad ; \quad \sigma_1 > 0, \quad \sigma_2 > 0 \ , \tag{19}$$

where, f_t is the uniaxial tensile strength of concrete. In the compression–tension stress state, the ultimate strength envelope can be expressed as

$$\begin{cases} f_2^{C.S} = \dfrac{1+3.28\beta}{(1+\beta)^2} f_c' \\ f_1^{C.S} = \beta f_2^{C.S} \end{cases} \quad ; \quad -0.17 \le \beta < 0 \tag{20}$$

$$\begin{cases} f_2^{C.S} = \dfrac{1+3.28\beta}{(1+\beta)^2} f_c' \\ f_1^{C.S} = \beta f_2^{C.S} \end{cases} \quad ; \quad -\infty \le \beta < -0.17 \ . \tag{21}$$

2.2.2. Nonlinear stress–strain relation in compression

To model the compressive behavior of concrete, as shown in Figure 3, a parabolic compressive hardening and softening model is used [10].

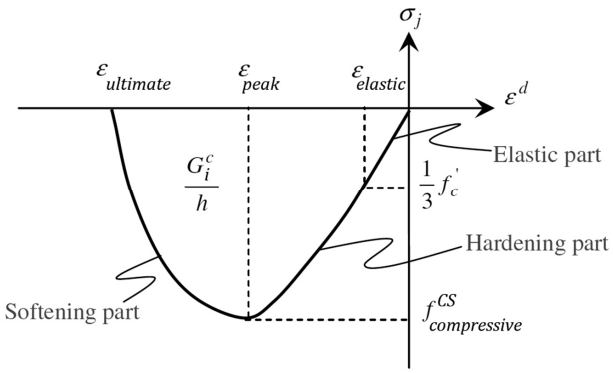

Figure 3. Nonlinear behavior of concrete in compression [10].

When concrete is loaded in compression, it is assumed that the stress–strain relation is linear up to the initial yield at the value of $(1/3)f_c'$, after which the stress–strain response is typically characterized by stress hardening followed by strain softening. The equivalent uniaxial stress–strain relation in compression is defined as

$$\sigma_i^{Current} = \begin{cases} E\varepsilon_i & \varepsilon_e \le \varepsilon_i \le 0 \\ \frac{f_c'}{3}\left[1 + 4\left(\frac{\varepsilon_i - \varepsilon_e}{\varepsilon_{p_i} - \varepsilon_e}\right) - 2\left(\frac{\varepsilon_i - \varepsilon_e}{\varepsilon_{p_i} - \varepsilon_e}\right)^2\right] & \varepsilon_{p_i} \le \varepsilon_i < \varepsilon_e \\ f_i^{C.S}\left[1 - \left(\frac{\varepsilon_i - \varepsilon_{p_i}}{\varepsilon_{u_i} - \varepsilon_{p_i}}\right)^2\right] & \varepsilon_{u_i} \le \varepsilon_i < \varepsilon_{p_i} \\ 0 & \varepsilon_i < \varepsilon_{u_i} \end{cases} \tag{22}$$

where, E is the Young's modulus of concrete and ε_i is the compressive strain. The strain ε_e is defined as

$$\varepsilon_e = \frac{1}{3}\frac{f_c'}{E} \tag{23}$$

The strain ε_p , at which the maximum compressive strength is reached, is defined as,

$$\varepsilon_{p_i} = \frac{4}{3}\frac{f_i^{C.S}}{E} + \varepsilon_e \tag{24}$$

in which, $f_i^{C.S}$ is the current compressive strength of concrete as defined by equations (18) to (21). Finally, the ultimate compressive strain ε_{u_i} is defined by

$$\varepsilon_{u_i} = \frac{3}{2}\frac{G_i^c}{h f_i^{C.S}} + \varepsilon_{p_i}, \tag{25}$$

where, G_i^c is the current compressive fracture energy of concrete, $f_i^{C.S}$ is the current compressive strength in the direction i and h is the crack band width. It could be assumed that the compressive fracture energy of concrete under biaxial stresses depends on its current compressive strength [7] using relation

$$G_i^c = \frac{(f_i^{C.S})_{Compressive}}{f_c'} G_c \tag{26}$$

in which, G_c is the uniaxial compressive fracture energy of concrete. For linear two–dimensional volumes, the crack band width h is defined as,

$$h = \sqrt{2A}, \tag{27}$$

where, A is the total area (of the control volume).

2.2.3. Nonlinear stress–strain relation in tension

The behavior of concrete in tension before cracking is assumed to be linear elastic. As it's shown in Figure 4, a fictitious crack model that is based on a linear softening curve and the Mode I fracture energy is adopted after cracking has occurred [11]. Thus, the equivalent uniaxial stress–strain relation in tension is assumed to be

$$\sigma_i^{Current} = \begin{cases} E\varepsilon_i & \varepsilon_{cr} \geq \varepsilon_i \geq 0 \\ f_t\left[1 - \left(\dfrac{\varepsilon_i - \varepsilon_{cr}}{\varepsilon_m - \varepsilon_{cr}}\right)^2\right] & \varepsilon_m \geq \varepsilon_i > \varepsilon_{cr} \\ 0 & \varepsilon_i > \varepsilon_m \end{cases}, \tag{28}$$

where, E is the Young's modulus of concrete, ε_i is the tensile strain, and f_t is the uniaxial tensile strength of concrete. The initial crack strain ε_{cr} is determined by

$$\varepsilon_{cr} = \frac{f_t}{E}, \tag{29}$$

the maximum crack strain ε_m is expressed as

$$\varepsilon_m = \frac{2G_f^I}{hf_t}, \tag{30}$$

in which G_f^I is the Mode I fracture energy, f_t is the tensile strength and h is the crack band width which is described in equation (27).

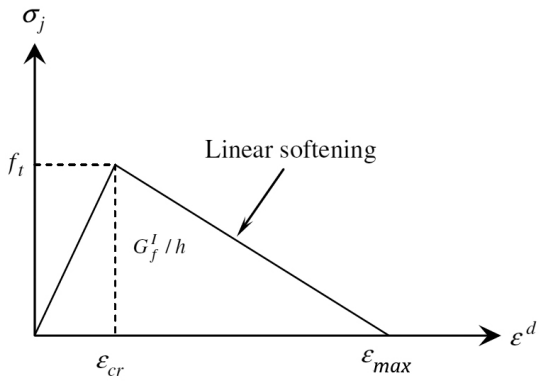

Figure 4. Nonlinear behavior of concrete in tension [11].

2.2.4. Secant stiffness matrix

When concrete is cracked or crushed, the Poisson's ratio is often set to zero, thus, the proposed model adopts a secant stiffness matrix that takes the form [7]

$$D = \begin{bmatrix} \overline{E_1} & 0 & 0 \\ 0 & \overline{E_2} & 0 \\ 0 & 0 & \bar{G} \end{bmatrix}, \tag{31}$$

with

$$\overline{E_1} = \frac{\sigma_1^{Current}}{\varepsilon_1^d}, \quad \overline{E_2} = \frac{\sigma_2^{Current}}{\varepsilon_2^d}, \quad \bar{G} = \frac{\overline{E_1 E_2}}{\overline{E_1} + \overline{E_2}}. \tag{32}$$

3. Numerical model

In this section, formulation of the GFVM (which does not require any matrix manipulations) is utilized to discretize the linear–elastic equations mentioned in sub–section 2.1. Thus, in order to ensure that the stability of iterative solution is provided, a proper time step limit is employed.

The intact nonlinear formulation mentioned in sub–section 2.2 is used to apply nonlinear behavior model of concrete under normal stresses. Noteworthy that, it is essential to utilize a load imposing technique for modeling the post–peak behavior of concrete (caused by the strain–softening phenomenon).

3.1. Galerkin finite volume method

In order to discretize the Cauchy's equilibrium equations, the following form is considered.

$$\rho \frac{\partial^2 u_i}{\partial t^2} = \overrightarrow{\nabla F_i}, \quad (j = 1, 2). \tag{33}$$

where, the components of the stress vector $\overrightarrow{F_i} = \sigma_{i1}\hat{\imath} + \sigma_{i2}\hat{\jmath}$ are defined as

$$\begin{aligned}
\sigma_{11} &= C_1\left(\frac{\partial u_x}{\partial x}\right) + C_2\left(\frac{\partial u_y}{\partial y}\right) + C_3\left(\frac{\partial u_x}{\partial y} + \frac{\partial u_y}{\partial x}\right), \\
\sigma_{12} &= C_3\left(\frac{\partial u_x}{\partial x}\right) + C_5\left(\frac{\partial u_y}{\partial y}\right) + C_6\left(\frac{\partial u_x}{\partial y} + \frac{\partial u_y}{\partial x}\right), \\
\sigma_{21} &= C_3\left(\frac{\partial u_x}{\partial x}\right) + C_5\left(\frac{\partial u_y}{\partial y}\right) + C_6\left(\frac{\partial u_x}{\partial y} + \frac{\partial u_y}{\partial x}\right), \\
\sigma_{22} &= C_2\left(\frac{\partial u_x}{\partial x}\right) + C_4\left(\frac{\partial u_y}{\partial y}\right) + C_5\left(\frac{\partial u_x}{\partial y} + \frac{\partial u_y}{\partial x}\right).
\end{aligned} \tag{34}$$

Following the concept of weighted residual method, multiplying the equation (33) by a weight function ω and integrating over sub–domain Ω end up with integral form of the equation as

$$\int_\Omega \omega \cdot \rho \frac{\partial^2 u_i}{\partial t^2} d\Omega = \int_\Omega \omega \cdot \left(\vec{\nabla} \cdot \overrightarrow{F_i}\right) d\Omega + \int_\Omega \omega \cdot b_i d\Omega \,. \tag{35}$$

In the absence of body forces, the terms containing spatial derivatives can be integrated by part over the sub–domain Ω and then the weak form of the equation (35) may be written as

$$\int_\Omega \omega \cdot \rho \frac{\partial^2 u_i}{\partial t^2} d\Omega = \left[\omega \cdot \overrightarrow{F_i}\right]_\Gamma - \int_\Omega \left(\overrightarrow{F_i} \cdot \vec{\nabla}\omega\right) d\Omega \,. \tag{36}$$

According to Galerkin weighted residual method, the weighting function ω can be chosen equal to the interpolation function ϕ. For a triangular type element with three nodes, the linear

interpolation function ϕ_k (which is called shape function in FEM), takes the value of unity at desired node n, and zero at other neighboring nodes on opposite side k (see Figure 5).

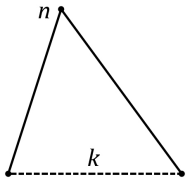

Figure 5. A linear triangular element.

Therefore, the summation of the term $\left[\omega \cdot \vec{F_i}\right]_\Gamma$, which is calculated over the boundary of sub–domain Ω, equals zero. So the right hand side of equation (36) can be discretized as

$$-\int_\Omega \left(\vec{F_i} \cdot \vec{\nabla}\omega\right) d\Omega = \frac{1}{2}\sum_{k=1}^{N} \left(\widetilde{F_i} \cdot \overrightarrow{\Delta l}\right)_k \tag{37}$$

where, $\overrightarrow{\Delta l}_k$ is the normal vector of the side k and $\widetilde{F_i}$ is the i direction piece wise constant stress vector at the center of element associated with the boundary side k.

Since linear triangular elements sharing a node form the desired sub–domain (see the computational control volume in Figure 6), the left hand side of equation (36) can be discretized as

$$\frac{\partial^2}{\partial t^2}\left(\int_\Omega \phi u_i d\Omega\right) \approx \frac{\Omega_n}{3}\frac{d^2 u_i}{dt^2}. \tag{38}$$

By applying the FDM concept in procedure of discretization of left hand side transient term, the time derivative of i direction displacement u_i in equation (36) can be discretized as

$$\rho\frac{\Omega_n}{3}\frac{d^2 u_i}{dt^2} = \rho\left(\frac{u_i^{t+\Delta t} - 2u_i^t + u_i^{t-\Delta t}}{(\Delta t)^2}\right)\frac{\Omega_n}{3}. \tag{39}$$

Eventually, using equations (38), (40) and (41), the discrete form of the Cauchy's equilibrium equations can be formulated as:

$$\left(\frac{u_i^{t+\Delta t} - 2u_i^t + u_i^{t-\Delta t}}{(\Delta t)^2}\right) = \frac{3\sum_{k=1}^{N}(\tilde{\sigma}_{i1}\Delta y - \tilde{\sigma}_{i2}\Delta x)_k}{2\rho\Omega_n} + \frac{b_i}{3\rho} \tag{40}$$

The σ_{ij} relations can be formulated in discrete form as

$$\begin{aligned}
\sigma_{xx} &= \frac{1}{A_k}\sum_{m=1}^{N}\left(C_1 u_x\Delta y - C_2 u_y\Delta x + C_3\left(u_x\Delta y - u_y\Delta x\right)\right)_k,\\
\sigma_{xy} = \sigma_{yx} &= \frac{1}{A_k}\sum_{m=1}^{N}\left(C_3 u_x\Delta y - C_5 u_y\Delta x + C_6\left(u_x\Delta y - u_y\Delta x\right)\right)_k,\\
\sigma_{yy} &= \frac{1}{A_k}\sum_{m=1}^{N}\left(C_2 u_x\Delta y - C_4 u_y\Delta x + C_5\left(u_x\Delta y - u_y\Delta x\right)\right)_k,
\end{aligned} \tag{41}$$

where, A_k is the area of triangular element associated with boundary side k of the sub–domain Ω_n (see Figure 6).

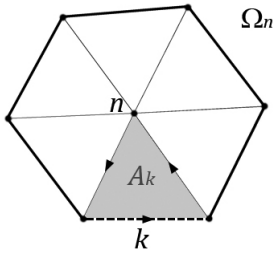

Figure 6. Triangular element with area A_k withinthe sub–domain Ω_n.

3.2. Computational iteration

In the iterative marching to the equilibrium conditions, it is necessary to select proper time step limit. So, that the stability of solution procedure is provided. For this purpose, the time step for solution of GFVM formulation of Cauchy equations on each control volume can be used as a limiting parameter for stabilizing the iterative marching of the computations to the equilibrium condition.

3.3. Load imposing technique

It's essential to utilize a load imposing technique which is capable of modeling the post–peak behavior of concrete, caused by the strain–softening phenomenon. Thus, by imposing displacement on the specimen and then calculating the equivalent load, the modeling of post–peak behavior is possible.

Since abrupt imposing external loads can lead to instability of numerical solution, a gradual load imposing technique which uses a relaxation coefficient $0 < C_{Relax} \leq 1$ during some computational iteration is implemented in the present model,

$$C_{Relax} = Min\left\{\left(\frac{I_{Step}}{L/\Delta t}\right), 1.0\right\}, \tag{42}$$

where, I_{Step} is the iteration number at the desired stage of the computation and L is a length scale that can be assumed as the distance between maximum displacement and the center of external load or constraint (support location).

In a realistically failed structure, we know that there are commonly several real open cracks that may lead to the failure of the structure. However, in the smeared rotating crack model, we often experience spurious cracking at a control volume center with a small crack strain. At the later loading stage, this control volume center may show unloading behavior, and may even load again. Furthermore, a realistic structure has the ability to redistribute stress after a crack opens, which similarly often leads to unloading in the concrete. It is therefore necessary to define the loading, unloading, and reloading behaviors of concrete.

In this paper, it's assumed that the cell which is cracked or crushed, will not gain any strength through the process of unloading or reloading (see Figure 7). It should be pointed out that the assumed unloading/reloading scheme is suitable for monotonic loading. However, for cyclic loading and the long–term response of concrete structures, a more realistic unloading/reloading scheme needs to be modeled.

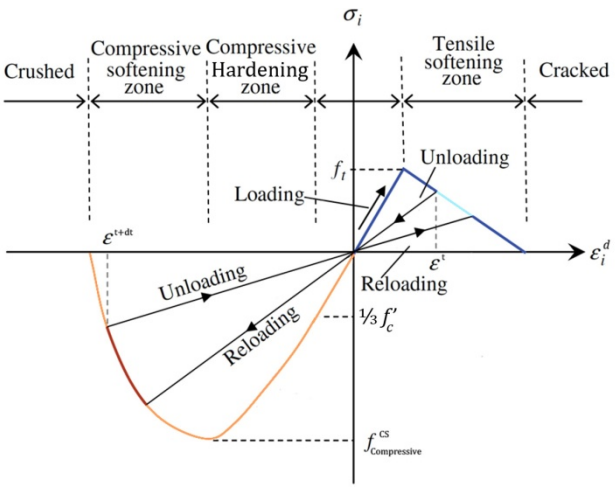

Figure 7. Loading–unloading–reloading scheme.

4. Computational results

In order to verify the accuracy of nonlinear GFVM solver, a 700×150×80 mm notched concrete beam with a notch of 50 mm (which simulates a crack) under three points bending is considered which. The properties of the specimen are tabulated in Table 1. Then, the results of nonlinear GFVM solver are compared with the available experimental measurements [12].

Table 1. Properties of concrete specimen.

Concrete Properties	Value
Density (ρ)	2403 $\frac{kg}{m^3}$
Modulus of Elasticity (E)	32 GPa
Poisson's Ratio (υ)	0.15
Compressive Strength (f_c')	58.3 MPa
Tensile Strength (f_t)	4.15 MPa
Compressive Fracture Energy (G_c)	175 kN/m
Tensile Fracture Energy (G_f)	164 N/m

In order to present the ability of the GFVM solver to deal with mesh refinement in the vicinity of the crack, an unstructured triangular mesh is utilized. The triangular mesh containing 1277 nodes and 2326 cells (triangular elements) which represents laboratory testing setup are shown in Figure 8.

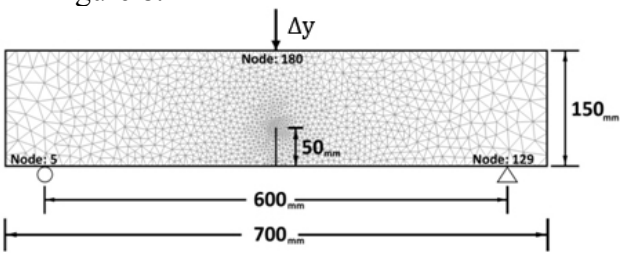

Figure 8. Numerical setup of the unstructured triangular mesh.

As mentioned before, the load is imposed by applying the displacement on the specimen. Thus, in an attempt to evaluate the equivalent load, it's essential to utilize the internal stresses induced by the imposed displacements. So, as it is shown in Figure 9, the equivalent load due to an imposed displacement can be computed as

$$P = -\left(R_{right} + R_{left}\right) = -H\left(-\tau_{xy}^{right} + \tau_{xy}^{left}\right) = H\left(\tau_{xy}^{right} - \tau_{xy}^{left}\right). \quad (43)$$

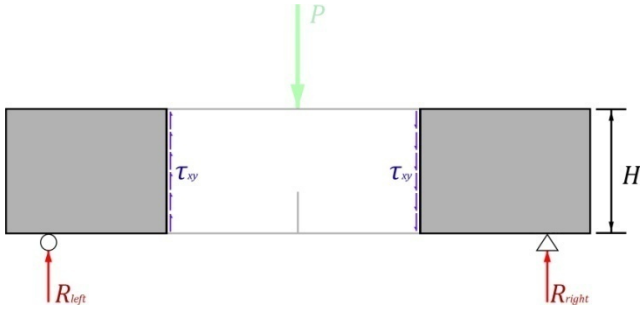

Figure 9. Evaluating equivalent load by using the internal stresses caused by an imposed displacement.

Through the numerical analysis and by the incremental displacement imposing, the cells of the mesh start to crack or crush and so their modulus of elasticity decrease. As shown in Figure 10, this reduction could represent the area of damaged material.

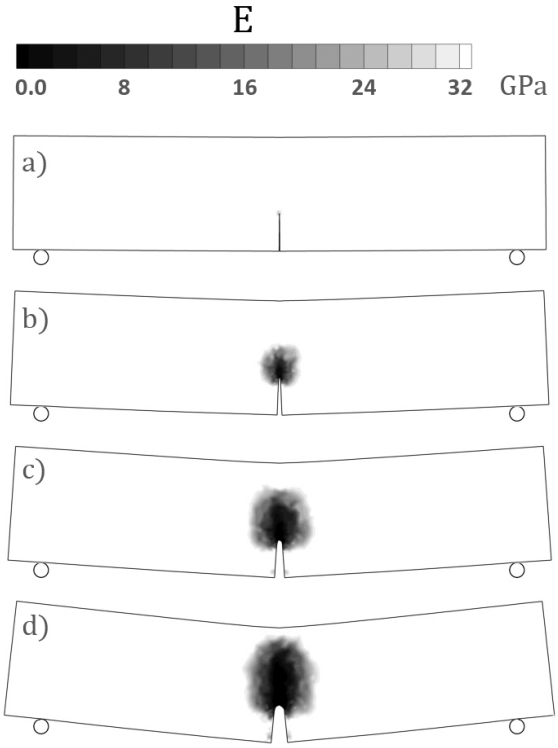

Figure 10. Gradual decrease of modulus of elasticity (from sample a to d) which represents the evolution of damage through the concrete beam.

The accuracy of the developed model is assessed by comparing the numerical and experimental envelope curve of monotonic load versus crack mouth opening displacement (CMOD) (see Figure 11). The maximum error of the computed results are calculated by evaluating the strain energy (integrating the CMOD curve as 0.4154) and comparing with integration of corresponding experimental measurement curve (0.4413), as

$$Err = \frac{|0.4154 - 0.4413|}{0.4154} = 6.02\% \quad (44)$$

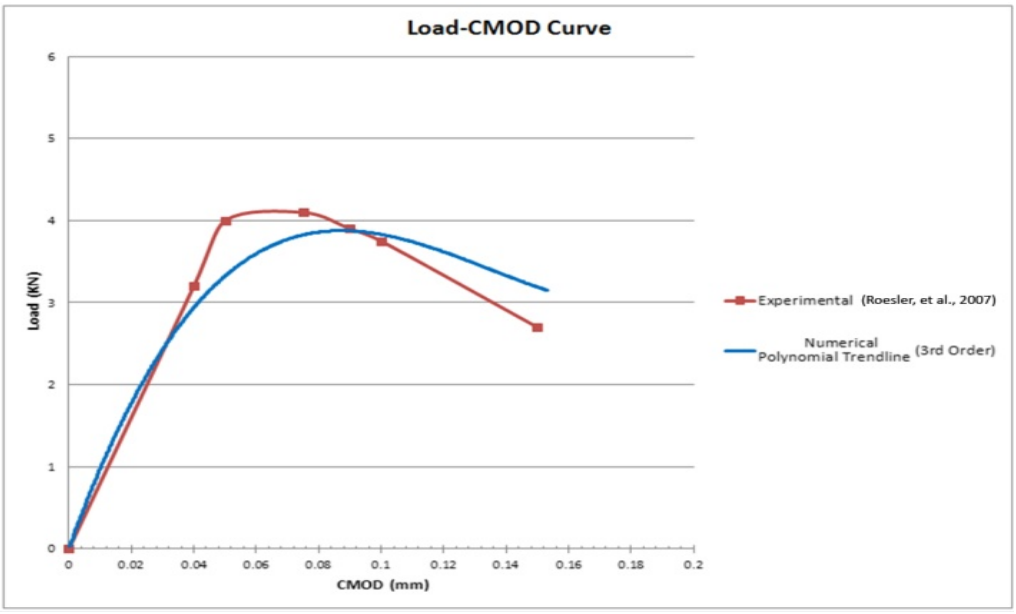

Figure 11. Comparison of numerical and experimental load–CMOD curve of notched concrete bean under three points bending.

5. Conclusion

In this paper, the vertex based Galerkin finite volume method (GFVM) for iterative solution of the two dimensional Cauchy equations is introduced and combined with the smeared rotating crack method (SRCM) in order to predict the nonlinear behavior of cracked concrete structures in equilibrium conditions.

The process of degradation caused by the incremental displacement imposing is simulated by reduction of modulus of elasticity of the cracked or crushed concrete cells (triangular elements).

The accuracy and performance of the developed GFVM solver is assessed by modeling a notched (cracked) beam under three point bending and then comparing numerical results with the reported experimental measurements.

The mesh refinement near a notch (crack) at the concrete beam is performed by adapting an unstructured rectangular mesh which the size of its cells were modified in accordance with the zone of stress concentration.

The computational results demonstrate that the introduced GFVM solver which considers two different sets of nonlinear stress–strain curves for handling the behavior of damaged concrete in both tension and compression can produce promising results.

It can be stated that, the present shape function free computational model solves stress and deformation of complicated problems of concrete structures without any matrix manipulations. The developed GFVM solver presents stable solution procedure with no artificial damping mechanism requirement and produces acceptable results.

The light computational work load of the GFVM iterative solver and its ability to deal with unstructured meshes make it suitable for applying to dynamic analysis of the concrete structures with complex geometrical features of the real world problems.

6. Aknowledgement

The first author would like to acknowledge Professor Soheil Mohammadi for his useful hints on the subject of this article and Civil Engineering Department of Tehran University for providing basic facilities for completing current paper.

References

[1] O.C. Zienkiewicz, R.L. Taylor, *The finite element method basic formulation and linear problems*, Vol.1, McGraw-Hill, Maidenhead (UK) 1989.
[2] I. Bijelonja, I. Demirdžić, S. Muzaferija, A finite volume method for incompressible linear elasticity, *Computer Methods in Applied Mechanics and Engineering*, Vol. 195 (2006) 6378-6390.
[3] A.K. Slone, C. Bailey, M. Cross, Dynamic solid mechanics using finite volume methods, *Applied Mathematical Modelling*, 27 (2003) 69-87.
[4] S.R. Sabbagh–Yazdi, N.E. Mastorakis, M. Esmaili, Explicit 2D matrix free galerkin finite volume solution of plane strain structural problems on triangular meshes, *International Journal of Mathematics and Computers in Simulation*, Vol. 1, 2 (2008) 1-8.
[5] S.R. Sabbagh–Yazdi, S. AliMohammadi, M.K. Pipelzadeh, Unstructured finite volume method for matrix–free explicit solution of stress–strain fields in two–dimensional problems with curved boundaries in equilibrium condition, *Applied Mathematical Modelling*, Vol. 36, 5 (2012) 2224–2236.
[6] Z.P. Bazant, B.H. Oh, Crack band theory for fracture of concrete, *RILEM Materials and Structures*, 93 (1983) 155–177.
[7] W. He, Y.F. Wu, K.M. Liew, Z. Wu, A 2D total strain based constitutive model for predicting the behaviors of concrete structures, *International Journal of Engineering Science*, 44 (2006) 1280–1303.
[8] R.J. Cope, P.V. Rao, Non-linear finite element analysis of concrete slab structures, *Proceedings of the Institution of Civil Engineers*, 63 (1977) 159-179.
[9] H. Kupfer, H.K. Hilsdorf, H. Rusch, Behavior of concrete under biaxial stresses, *Journal of the American Concrete Institute,* 66 (1969) 656–666.
[10] R.A. Vonk, Softening of concrete loaded in compression, *Ph.D. Thesis*, Eindhoven University of Technology, Eindhoven, 1992.
[11] U.A. Ebead, H. Marzouk, Tension-Stiffening Model for FRP-Strengthened Concrete Two-Way Slabs, *RILEM Materials and Structures*, 276 (2005) 193–200.
[12] J. Roesler, G.H. Paulino, K. Park, C. Gaedicke, Concrete Fracture Prediction Using Bilinear Softening, *Cement & Concrete Composites*, 29 (2007) 300–312.